JOC Article
pubs.acs.org/joc

DFT Study on the Factors Determining the Enantioselectivity of Friedel−Crafts Reactions of Indole with *N*-Acyl and *N*-Tosylimines Catalyzed by BINOL−Phosphoric Acid Derivatives

Luis Simón[†] and Jonathan M. Goodman*[,‡]

[†]*Facultad de Ciencias Químicas, Universidad de Salamanca, Plaza de los Caídos 1-5, Salamanca, E37004, Spain and* [‡]*Unilever Centre For Molecular Science Informatics, Department of Chemistry, Lensfield Road, Cambridge, CB2 1EW, U.K.*

jmg11@cam.ac.uk

Received October 2, 2009

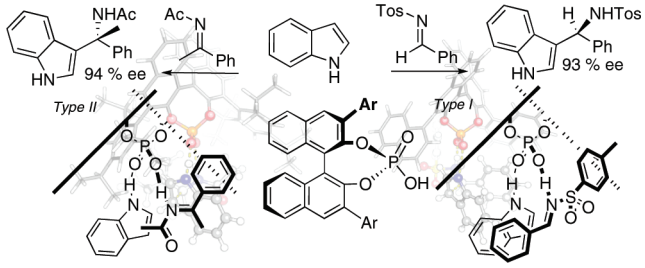

DFT methods have been used to study the mechanism and the enantioselectivity of the Friedel−Crafts reaction of indoles with acyl and tosyl imides catalyzed by BINOL−phosphoric acid catalysts. The results are in excellent agreement with the experimental enantioselectivities. The energies of the competing transition structures and, thus, the enantioselectivity are rationalized from calculations on a model system. We propose a simple model to predict the absolute configuration of the products.

Introduction

BINOL−phosphoric acid derivatives are highly versatile enantioselective catalysts in many organic reactions.[1] Their most common application is the catalysis of nucleophilic additions to imines, but they have recently been used in many other processes. Examples include reactions with aziridines,[2,3] additions of enamide to in situ generated carbocations,[4] dipolar cycloadditions between azomethine ylides and methyleneindolinones,[5] hetero-Diels−Alder reactions on glyoxylate,[6] Michael addition to enones, Robinson-type annulation,[7] and hydroxylation of β-keto esters using nitroso compounds.[8] They have also been used successfully to catalyze reduction processes, including Hantzsch ester[9−27]

*To whom correspondence should be addressed. Tel: +44 (0)1223. Fax: +44 (0)1223 763076.

(1) Terada, M. *Cemm. Commun.* **2008**, 4097–4112.
(2) Sala, G. D.; Lattanzi, A. *Org. Lett.* **2009**, *11*, 3330–3333.
(3) Rowland, E. B.; Rowland, G. B.; Rivera-Otero, E.; Antilla, J. C. *J. Am. Chem. Soc.* **2007**, *129*, 12084–12085.
(4) Guo, Q.-X.; Peng, Y.-G.; Zhang, J.-W.; Song, L.; Feng, Z.; Gong, L.-Z. *Org. Lett.* **2009**, *11*, 4620–4623.
(5) Chen, X.-H.; Wei, Q.; Luo, S.-W.; Xiao, H.; Gong, L.-Z. *J. Am. Chem. Soc.* **2009**, *131*, 13819–13825.
(6) Momiyama, N.; Tabuse, H.; Terada, M. *J. Am. Chem. Soc.* **2009**, *131*, 12882–12883.
(7) Akiyama, T.; Katoh, T.; Mori, K. *Angew. Chem., Int. Ed.* **2009**, *48*, 4226–4228.
(8) Lu, M.; Zhu, D.; Lu, Y.; Zeng, X.; Tan, B.; Xu, Z.; Zhong, G. *J. Am. Chem. Soc.* **2009**, *131*, 4562–4563.
(9) Rueping, M.; Sugiono, E.; Azap, C.; Theissmann, T.; Bolte, M. *Org. Lett.* **2005**, *7*, 3781–3783.
(10) Hoffmann, S.; Nicoletti, M.; List, B. *J. Am. Chem. Soc.* **2006**, *128*, 13074–13075.
(11) Rueping, M.; Antonchick, A. P.; Theissmann, T. *Angew. Chem., Int. Ed.* **2006**, *45*, 3683–3686.
(12) Rueping, M.; Antonchick, A. P.; Theissmann, T. *Angew. Chem., Int. Ed.* **2006**, *45*, 6751–6755.
(13) Storer, R. I.; Carrera, D. E.; Ni, Y.; MacMillan, D. W. C. *J. Am. Chem. Soc.* **2006**, *128*, 84–86.
(14) Yang, J. W.; List, B. *Org. Lett.* **2006**, *8*, 5653–5655.
(15) Li, G.; Liang, Y.; Antilla, J. C. *J. Am. Chem. Soc.* **2007**, *129*, 5830–5831.
(16) Zhou, J.; List, B. *J. Am. Chem. Soc.* **2007**, *129*, 7498–7499.
(17) Hoffmann, S.; Seayad, A. M.; List, B. *Angew. Chem., Int. Ed.* **2005**, *44*, 7424–7427.
(18) Rueping, M.; Antonchick, A. P. *Angew. Chem., Int. Ed.* **2007**, *46*, 4562–4565.
(19) Guo, Q.-S.; Du, D.-M.; Xu, J. *Angew. Chem., Int. Ed.* **2008**, *47*, 759–762.
(20) Li, G.; Antilla, J. C. *Org. Lett.* **2009**, *11*, 1075–1078.
(21) Rueping, M.; Antonchick, A. P. *Angew. Chem., Int. Ed.* **2008**, *47*, 5836–5838.

DOI: 10.1021/jo902120s Published on Web 12/29/2009

reduction, benzothiazoline[28] reduction, and metal-cocatalyzed reductive amination.[29] A wide range of nucleophiles are compatible with this catalyst, making it possible to do asymmetric Strecker reactions,[30−32] Mannich reactions,[33−39] hetero-Diels−Alder reactions,[40−42] dipolar cycloadditions,[43−45] and alcohol,[46] phosphite,[47] alkyne,[48] isocyanide,[49] and amino[50,51] additions to imines. In addition, aza-ene-type reactions,[52−55] aza-Petasis−Ferrier rearrangement,[56] acylcyanations,[57] conjugated additions,[11,16,19,22,58,59] Pictet−Spengler,[60,61] aza-Darzens,[62] enamide self-condensation,[63] and Friedel−Crafts[64−70] reactions are also catalyzed effectively. For the additions to imines, the reactions can be divided into three classes: those in which *N*-phenylimines derived from ketones[9,11−13,15−17,19,22−29,50] or from aldehydes[10,33,34,36,37,40,47−49,51,58,69−71] are used; those in which *N*-benzylimines[21,30,31] are employed; and those in which *N*-tosyl[64,72−74] and *N*-acyl[20,35,39,46,52,53,55,56,63,65−68,75] imines are the starting materials.

In his work on the hydrophosphonylation of imines,[47] Akiyama proposed a concerted mechanism in which the BINOL phosphoric acid catalyst acted simultaneously as an acid (protonating the imine) and as a base (toward the phosphite). This mechanism has also been proposed for the Friedel−Crafts reaction of indoles,[65] Mannich reaction,[34] or aza-ene-type reaction.[52] At almost the same time, Rueping proposed a stepwise catalytic cyclic mechanism for the Hantzsch ester reduction of imines[9,11,12] in which the BINOL−phosphoric acid catalyst first protonates the imine, facilitating the nucleophilic attack and yielding the protonated nucleophile that regenerates the catalyst in a protonation step. The enantioselectivity of the reaction was explained by considering the possible geometry of the iminium−phosphate complex.[9,11−13,30] Terada has suggested an explanation for the enantioselectivity of a Mannich reaction based on calculations and ^{1}H NMR analysis of the reactive complex.[76] Using computational methods, we have recently found that the most plausible mechanism for both the Hantzsch ester hydrogenation[77] and the Strecker reaction[78] of imines, using BINOL−phosphoric acid catalysts, is a concerted mechanism. Independently, Himo has arrived at similar conclusions for Hantzsch ester hydrogenations,[79,80] and this concerted mechanism is usually used in the most recent literature.[1,20,70,71] Most recently, calculations on the

(22) Kang, Q.; Zhao, Z.-A.; You, S.-L. *Org. Lett.* **2008**, *10*, 2031–2034.
(23) Kang, Q.; Zhao, Z.-A.; You, S.-L. *Adv. Synth. Catal.* **2007**, *349*, 1657–1660.
(24) Rueping, M.; Theissmann, T.; Raja, S.; Bats, J. W. *Adv. Synth. Catal.* **2008**, *350*, 1001–1006.
(25) Schrader, W.; Handayani, P. P.; Zhou, J.; List, B. *Angew. Chem., Int. Ed.* **2009**, *48*, 1463–1466.
(26) Han, Z.-Y.; Xiao, H.; Chen, X.-H.; Gong, L.-Z. *J. Am. Chem. Soc.* **2009**, *131*, 9182–9183.
(27) Liu, X.-Y.; Che, C.-M. *Org. Lett.* **2009**, *11*, 4204–4207.
(28) Zhu, C.; Akiyama, T. *Org. Lett.* **2009**, *11*, 4180–4183.
(29) Li, C.; Villa-Marcos, B.; Xiao, J. *J. Am. Chem. Soc.* **2009**, *131*, 6967–6969.
(30) Rueping, M.; Sugiono, E.; Azap, C. *Angew. Chem., Int. Ed.* **2006**, *45*, 2617–2619.
(31) Rueping, M.; Sugiono, E.; Moreth, S. A. *Adv. Synth. Catal.* **2007**, *349*, 759–764.
(32) Shen, K.; Liu, X.; Cai, Y.; Lin, L.; Feng, X. *Chem.—Eur. J.* **2009**, *15*, 6008–6014.
(33) Yamanaka, M.; Itoh, J.; Fuchibe, K.; Akiyama, T. *J. Am. Chem. Soc.* **2007**, *129*, 6756–6764.
(34) Guo, Q.-X.; Liu, H.; Guo, C.; Luo, S.-W.; Gu, Y.; Gong, L.-Z. *J. Am. Chem. Soc.* **2007**, *129*, 3790–3791.
(35) Uraguchi, D.; Terada, M. *J. Am. Chem. Soc.* **2004**, *126*, 5356–5357.
(36) Akiyama, T.; Itoh, J.; Yokota, K.; Fuchibe, K. *Angew. Chem., Int. Ed.* **2004**, *43*, 1566–1568.
(37) Sickert, M.; Schneider, C. *Angew. Chem., Int. Ed.* **2008**, *47*, 3631–3634.
(38) Ting, A.; Schaus, S. E. *Eur. J. Org. Chem.* **2007**, *2007*, 5797–5815.
(39) Terada, M.; Machioka, K.; Sorimachi, K. *Angew. Chem., Int. Ed.* **2009**, *48*, 2553–2556.
(40) Liu, H.; Cun, L.-F.; Mi, A.-Q.; Jiang, Y.-Z.; Gong, L.-Z. *Org. Lett.* **2006**, *8*, 6023–6026.
(41) Akiyama, T.; Tamura, Y.; Itoh, J.; Morita, H.; Fuchibe, K. *Synlett* **2006**, *1*, 141–143.
(42) Jiang, J.; Qing, J.; Gong, L.-Z. *Chem.—Eur. J.* **2009**, *15*, 7031–7034.
(43) Jiao, P.; Nakashima, D.; Yamamoto, H. *Angew. Chem., Int. Ed.* **2008**, *47*, 2411–2413.
(44) Chen, X.-H.; Zhang, W.-Q.; Gong, L.-Z. *J. Am. Chem. Soc.* **2008**, *130*, 5652–565.
(45) Liu, W.-J.; Chen, X.-H.; Gong, L.-Z. *Org. Lett.* **2008**, *10*, 5357–5360.
(46) Li, G.; Fronczek, F. R.; Antilla, J. C. *J. Am. Chem. Soc.* **2008**, *130*, 12216–12217.
(47) Akiyama, T.; Morita, H.; Itoh, J.; Fuchibe, K. *Org. Lett.* **2005**, *7*, 2583–2585.
(48) Rueping, M.; Antonchick, A. P.; Brinkmann, C. *Angew. Chem., Int. Ed.* **2007**, *46*, 6903–6906.
(49) Yue, T.; Wang, M.-X.; Wang, D.-X.; Masson, G.; Zhu, J. *Angew. Chem., Int. Ed.* **2009**, *48*, 6717–6721.
(50) Cheng, X.; Vellalath, S.; Goddard, R.; List, B. *J. Am. Chem. Soc.* **2008**, *130*, 15786–15787.
(51) Rueping, M.; Antonchick, A. P.; Sugiono, E.; Grenader, K. *Angew. Chem., Int. Ed.* **2008**, *48*, 908–910.
(52) Terada, M.; Machioka, K.; Sorimachi, K. *Angew. Chem., Int. Ed.* **2006**, *45*, 2254–2257.
(53) Terada, M.; Machioka, K.; Sorimachi, K. *J. Am. Chem. Soc.* **2007**, *129*, 10336–10337.
(54) Terada, M.; Soga, K.; Momiyama, N. *Angew. Chem., Int. Ed.* **2008**, *47*, 4122–4125.
(55) Rueping, M.; Sugiono, E.; Theissmann, T.; Kuenkel, A.; Kockritz, A.; Pews-Davtyan, A.; Nemati, N.; Beller, M. *Org. Lett.* **2007**, *9*, 1065–1068.
(56) Terada, M.; Toda, Y. *J. Am. Chem. Soc.* **2009**, *131*, 6354–6355.
(57) Pan, S. C.; Zhou, J.; List, B. *Angew. Chem., Int. Ed.* **2007**, *46*, 612–614.
(58) Jiang, J.; Yu, J.; Sun, X.-X.; Rao, Q.-Q.; Gong, L.-Z. *Angew. Chem., Int. Ed.* **2008**, *47*, 2458–2462.
(59) Rueping, M.; Theissmann, T.; Antonchick, A. P. *Synlett* **2006**, 1071–1074.
(60) Wanner, M. J.; van der Haas, R. N. S.; de Cuba, K. R.; van Maarseveen, J. H.; Hiemstra, H. *Angew. Chem., Int. Ed.* **2007**, *46*, 7485–7487.
(61) Wanner, M. J.; Boots, R. N. A.; Eradus, B.; Gelder, R. d.; van Maarseveen, J. H.; Hiemstra, H. *Org. Lett.* **2009**, *11*, 2579.
(62) Akiyama, T.; Suzuki, T.; Mori, K. *Org. Lett.* **2009**, *11*, 2445–2447.
(63) Baudequin, C.; Zamfir, A.; Tsogoeva, S. B. *Chem. Commun.* **2008**, 4637–4639.
(64) Kang, Q.; Zhao, Z.-A.; You, S.-L. *J. Am. Chem. Soc.* **2007**, *129*, 1484–1485.
(65) Jia, Y.-X.; Zhong, J.; Zhu, S.-F.; Zhang, C.-M.; Zhou, Q.-L. *Angew. Chem., Int. Ed.* **2007**, *46*, 5565–5567.
(66) Li, G.; Rowland, G. B.; Rowland, E. B.; Antilla, J. C. *Org. Lett.* **2007**, *9*, 4065–4068.
(67) Terada, M.; Sorimachi, K. *J. Am. Chem. Soc.* **2007**, *129*, 292–293.
(68) Terada, M.; Yokoyama, S.; Sorimachi, K.; Uraguchi, D. *Adv. Synth. Catal.* **2007**, *349*, 1863–1867.
(69) Kang, Q.; Zhao, Z.-A.; You, S.-L. *Tetrahedron* **2009**, *65*, 1603–1607.
(70) Zhang, G.-W.; Wang, L.; Nie, J.; Ma, J.-A. *Adv. Synth. Catal.* **2008**, *350*, 1457–1463.
(71) Liu, H.; Dagousset, G.; Masson, G.; Retailleau, P.; Zhu, J. *J. Am. Chem. Soc.* **2009**, *131*, 4598–4599.
(72) Shi, Y.-L.; Shi, M. *Adv. Synth. Catal.* **2007**, *349*, 2129–2135.
(73) Kang, Q.; Zheng, X.-J.; You, S.-L. *Chem.—Eur. J.* **2008**, *14*, 3539–3542.
(74) Hou, Z.; Wang, J.; Liu, X.; Feng, X. *Chem.—Eur. J.* **2008**, *14*, 4484–4486.
(75) Hashimoto, T.; Maruoka, K. *J. Am. Chem. Soc.* **2007**, *129*, 10054–10055.
(76) Gridnev, I. D.; Kouchi, M.; Sorimachi, K.; Terada, M. *Tetrahedron Lett.* **2007**, *48*, 497–500.
(77) Simón, L.; Goodman, J. M. *J. Am. Chem. Soc.* **2008**, *130*, 8741–8747.
(78) Simón, L.; Goodman, J. M. *J. Am. Chem. Soc.* **2009**, *131*, 4070–4077.
(79) Marcelli, T.; Hammar, P.; Himo, F. *Chem.—Eur. J.* **2008**, *14*, 8562–8571.
(80) Marcelli, T.; Hammar, P.; Himo, F. *Adv. Synth. Catal.* **2009**, *351*, 525–529.

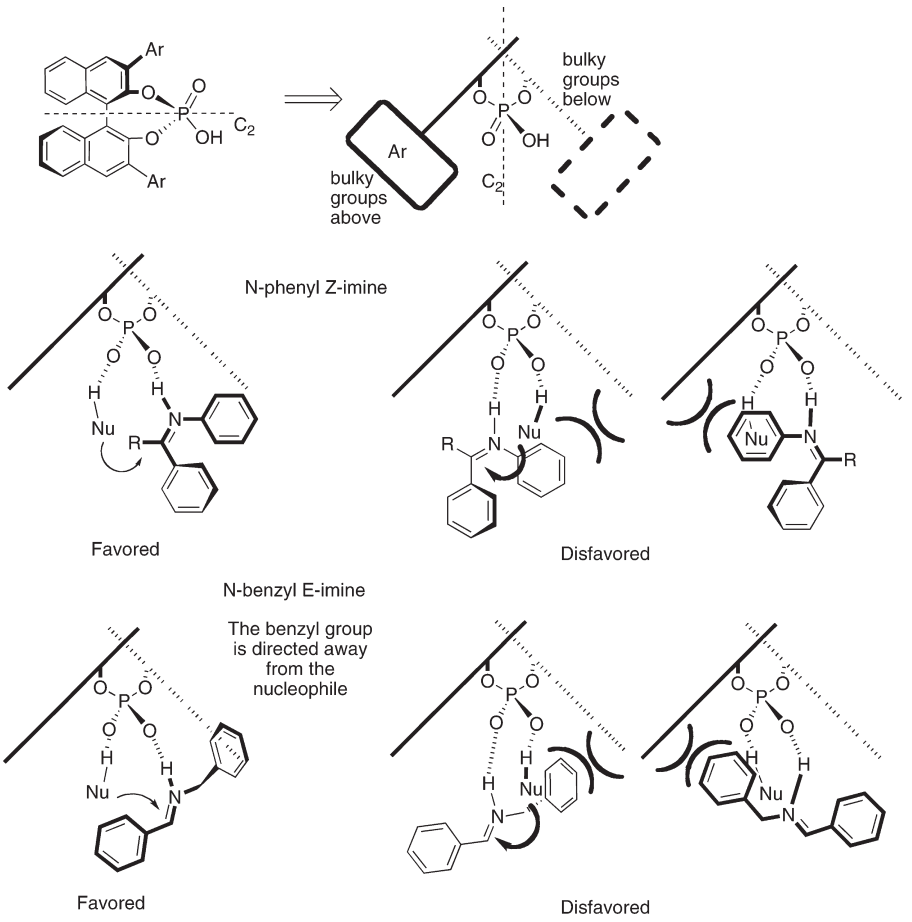

FIGURE 1. Model to predict the enantioselectivity of the BINOL−phosphoric catalyzed reactions applied to ketone *N*-phenylimines (*Z* conformation preferred) and to aldehyde *N*-benzylimines (*E* conformation preferred).

hydrophosphonylation of imines by Akiyama and Yamanaka,[81] Song,[82] and Yamanaka[83] also suggest a concerted mechanism.

The concerted mechanism, in turn, can explain the high enantioselectivity typically observed in these reactions. The catalyst simultaneously establishes H-bond interactions with the nucleophile and the electrophile. The steric effects of the bulky BINOL−phosphoric acid substituents give rise to a third interaction. Therefore, the three-point interaction model,[84] which is often invoked to explain chiral recognition phenomena,[85] can be applied here to explain the discrimination of the catalyst for the two possible enantiomeric transition states. Based on the observation of the transition state geometries, we proposed a simple model for predicting the enantioselectivity of the reaction[77,78] (Figure 1). According to this model, the BINOL−phosphoric acid catalyst is drawn so C_2 symmetry axis is in the plane of the paper and acid and basic phosphoric oxygen atoms are placed over and below this plane. In such a representation, bulky catalyst groups are placed over and below the paper at different sides of the C_2 axis. Therefore, when nucleophile and imine interact with the phosphate oxygen atoms, in the most stable transition state steric interactions are minimized but not in the transition state corresponding to the minor product. In order to explain the right enantioselectivity, it is necessary to consider the conformation of the electrophile, which depends on the shape of the substrate: *N*-phenyl ketone imines prefer a *Z* conformation in the transition state,[77] but *N*-benzyl aldehyde imines adopt an *E* conformation.[78]

In this paper, we study the factors contributing to the enantioselectivity of the Friedel−Crafts reaction of indole to *N*-acylimines derived from ketones and *N*-tosylimines derived from aldehydes. *N*-Acylimines are very interesting substrates for these reactions, since some of them can be readily transformed in the corresponding imines (*N*-Boc- or *N*-Cbz-imines, for example). Unlike Hantzsch ester or hydrogen cyanide, indole is an unsymmetrical and large nucleophile, so steric interactions with the catalysts might also play a role in the final enantioselectivity. There are a number of examples in the literature in which this kind of catalyst is successfully employed. We have focused on the reaction of *N*-acetylacetophenone imine, published by Zhou[65] (Figure 2), and the reaction on *N*-tosylimine derived from benzaldehyde published by You.[64] In the first reaction the acyl imine is generated in situ starting from the corresponding acyl enamine. In a similar reaction, Terada[67] showed that this tautomerization might be the reaction rate-determining step but has no effect on the final enantioselectivity of the reaction. The final tautomerization step of

(81) Akiyama, T.; Morita, H.; Bachu, P.; Mori, K.; Yamanaka, M.; Hirata, T. *Tetrahedron* **2009**, *65*, 4950–4956.
(82) Shi, F.-Q.; Song, B.-A. *Org. Biom. Chem.* **2009**, *7*, 1292–1298.
(83) Yamanaka, M.; Hirata, T. *J. Org. Chem.* **2009**, *74*, 3266–3271.
(84) Easson, L. H.; Stedman, E. *J. Biochem.* **1933**, *27*, 1257–1266.
(85) Vadim, A. D. *Chirality* **1997**, *9*, 99–102.

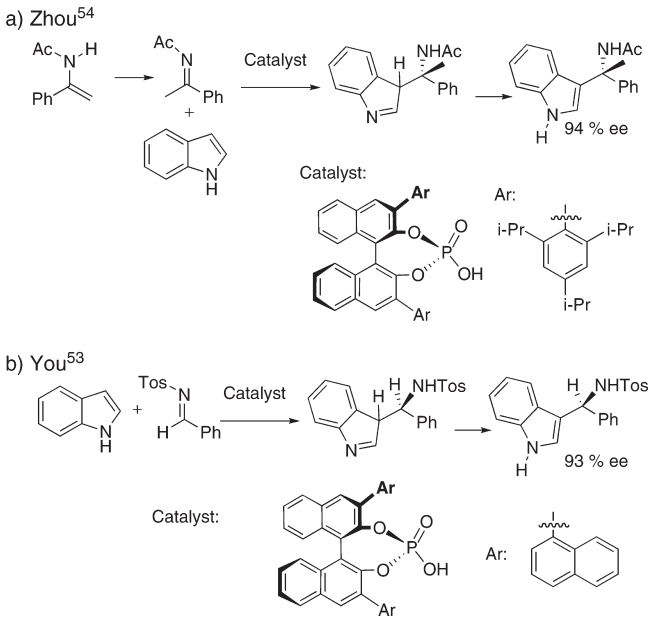

FIGURE 2. Reactions studied in this work: (a) *N*-acetyl acetophenone imine Friedel–Crafts reaction studied by Zhou;[54] (b) *N*-tosyl acetaldehyde reaction studied by You.[53] The enantiomeric series was chosen for study for consistency with our earlier work. In (a), the indole attacks from behind, as drawn, and in (b) the indole attacks from the front.

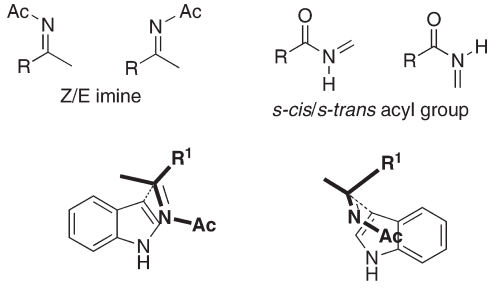

FIGURE 3. Competing conformations for the transition state of the reactions.

the Friedel–Crafts reaction, that regenerates the indole ring, takes place after the selective addition to the imine and has no effect on the enantioselectivity. Therefore, as we are interested in the factors that determine the reaction enantioselectivity, we have studied only the addition step of the process.

Results and Discussion

Reaction between Indole and Acyl Imines. In order to ensure that all transition-state geometries were included in the study, an exhaustive conformational search was required. *Z* and *E* conformations of the imine and *s-trans* and *s-cis* conformations of the acyl group need to be considered, as well as two possible relative orientations of the indole and the electrophile (Figure 3). This latter possibility arises as a consequence of the lack of symmetry of the nucleophile, and was not present in our studies of Hantzsch ester or hydrogen cyanide reactions. In addition, for each conformer, two possible diastereomeric transition states are possible, each leading to a different product enantiomer (*R* or *S*, obtained with the *R* absolute configuration in the catalyst). Overall, the calculation of 16 transition structures for each reaction is required. The relative contributions to the final product of each transition structure were calculated according to a Maxwell–Boltzmann distribution, using the Gibbs free energy and the temperature reported in the experiments (see the Computational Details). The enantiomeric excess of each reaction was calculated adding up contributions corresponding to each product enantiomer. Using this method, the enantiomeric excess calculated for the reaction of *N*-acetylacetophenone imine was 97%, in good agreement with the result obtained experimentally by Zhou[65] (94% ee).

A schematic summary of the transition states found is shown in Scheme 1. In general, transition structures in which the acyl group shows an *s-cis* conformation are lower in energy than those in which this group is *s-trans*. *E*-Imine conformation is also preferred over *Z*-imine conformation, and the transition structures in which the indole aromatic ring is in van der Waals contact with the acyl group are more stable than those in which this group changes its orientation. Interactions with the catalyst groups are responsible for the energy differences of the *R* and *S* product for each conformation studied.

Different conformations of the imine substrate and different orientations of the indole ring affect the energy of the resulting transition structures, but energy differences will also be influenced by the presence of steric interactions with the catalyst. In order to investigate both effects, we have calculated the transition structures when the BINOL–phosphoric acid catalyst was substituted by buta-1,3-diene-1,4-diol–phosphoric acid. This simplified model of the catalyst lacks the bulky groups, and therefore, the transition structures should be reasonably free of steric interactions. In agreement with the calculations in which the full structure of the catalyst was included, the most stable transition structure corresponds to an *E*-imine in which acyl group has an *s-cis* conformation and in which the indole ring is oriented toward the *N*-acyl substituent (TS1-*E*-*s*-*cis*-end, Scheme 1).

E/*Z* relative stability is an important factor for deciding the stereochemical outcome of the reaction, since reaction with the *Z* conformer yields the opposite enantiomer to the reaction with the *E* conformer. *E*/*Z* isomerization of imines would be a slow process if it were to occur via an in-plane inversion.[86] However, as the first step of the reaction is the tautomerization of the acyl enamine to the acyl imine, both *E* and *Z* imine conformers can be readily obtained. Calculations with the simplified model of the catalyst reveal that the *E* transition structure is 7.8 kcal/mol more stable than the *Z* transition state, an energy difference larger than that observed when the complete structure of the catalyst is included (difference between TS1-*E*-*s*-*cis*-end(*R*) and TS1-*Z*-*s*-*cis*-end(*S*): 2.7 kcal/mol). This can be explained after considering that *Z*-imine show a more compact structure in TS1-*E*-*s*-*cis*-end(*S*), and, therefore, steric interactions with the catalyst are reduced.

The comparison is performed between TS1-*E*-*s*-*cis*-end(*R*) and TS1-*Z*-*s*-*cis*-end(*S*) structures since the only difference

(86) Banik, B. K.; Lecea, B.; Arrieta, A.; de Cózar, A.; Cossío, F. P. *Angew. Chem., Int. Ed.* **2007**, *46*, 9347–9438.

SCHEME 1. Different Geometries of Transition Structures Studied for the *N*-Acylimine Reaction[a]

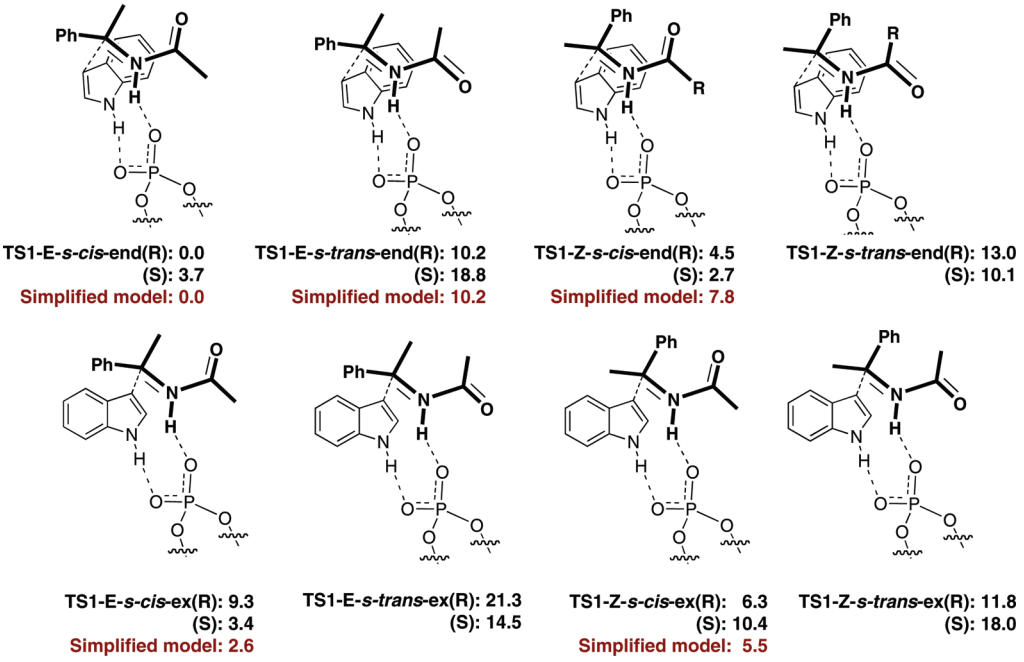

[a]The *R* and *S* in the names refer to the product. The *R* catalyst was used in all cases. $\Delta\Delta G$ (in toluene) are expressed in kcal/mol.

between these structures is the imine conformation. As previously discussed, this difference will lead to opposite enantiomers, but the interactions with the bulky catalyst groups are similar for both structures. A similar comparison could be made between TS1-*E*-*s*-*cis*-end(*S*) and TS1-*Z*-*s*-*cis*-end(*R*) where the energy difference is 0.8 kcal/mol.

The energy differences between the *E* and *Z* conformations in the simplified model transition states are so large than not even the catalyst's steric interactions can change the preference for the *E* transition state, and the contributions of the *Z* ones to the final product are negligible. This preference contrasts with our observations for the reaction of *N*-phenylimines with Hantzsch esters, where the *Z*-imine transition state was more stable by around 2.9 kcal/mol in the case of the simplified catalyst model and the stability was further increased when the bulky groups of the catalyst were included.[77] This preference has also been confirmed by independent studies performed by Himo et al.[79] In our study of the Strecker reaction on *N*-benzylimines, we found that *Z*-imine transition structures were also preferred for the acetophenone-derived imine but in the reactions of benzaldehyde-derived imine transition structures containing the *E* conformation show lower energy.[78] Therefore, it seems clear that the energy dependence on the *Z*/*E*-imine conformation of the transition structure depends on the nitrogen substituent, and the highest preference for *E*-imine conformation is obtained for *N*-acylimines. Ground-state calculations of the *Z*/*E* preference can give a clear indication of the transition-state preferences.

The results in Scheme 1 also establish the preference for the *s*-*cis* conformation of the imine acyl: 10.2 kcal/mol difference between TS1-*E*-*s*-*cis*-end(*R*) and TS1-*E*-*s*-*trans*-end(*R*) structures. This energy difference matches that calculated for the catalyst model with no bulky substituents (10.2 kcal/mol). The steric effects of the catalyst is unlikely, therefore, to affect the *s*-*cis*/*s*-*trans* preference to any significant extent.

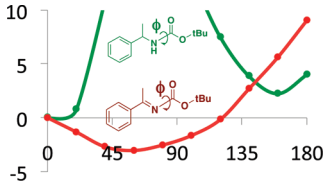

FIGURE 4. Geometry optimization scans (electronic energy, kcal mol^{-1}, B3LYP/6-31G*(*)//MPWB1K/6-31G**) of amides and acyl imines as a function of dihedral angle ϕ.

The preference for the *s*-*cis* conformation of the imine in the transition state could be related to a similar trend in the imine or the amide products since the transition state shares some characteristics with the reactants and products. To investigate this, we have performed relaxed geometry scans for the corresponding acyl-imines and amides, in which the O=C−N=R dihedral angle was fixed and the rest of geometrical parameters were optimized. The results are shown in Figure 4. As expected, the less stable conformation of the amide is that in which the dihedral angle is close to 90°, since this removes resonance stabilization of the amide. Dihedral angles close to 180° are also less stable than conformations where this angle is close to 0°. This is in agreement with previous observations of the higher stability of *Z* amides (ϕ = 0°) with respect to *E* amides (ϕ = 180°).[87] The energy differences observed here are also consistent with the literature.[87] For the acyl imine, the energy difference between the *s*-*cis* (ϕ = 0°) and *s*-*trans* (ϕ = 180°) conformations is higher; steric interactions between the acyl and acetophenone methyl groups contribute to the higher energy of the *S*-*trans*

(87) Avalos, M.; Babiano, R.; Barneto, J. L.; Bravo, J. L.; Cintas, P.; Jimenez, J. L.; Palacios, J. C. *J. Org. Chem.* **2001**, *66*, 7275–7282.

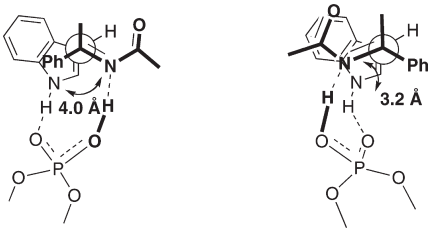

FIGURE 5. Geometrical differences in the transition structure for different indole orientations.

conformation. Steric interactions between the acyl oxygen and acetophenone methyl group are also responsible for the higher stability of a *gauche* (ϕ = 60°) conformation. The *S-cis* conformation is about 10 kcal/mol more stable than the *S-trans* conformation. These results show that the contribution to the energy of the transition structures of the *S-cis*/*S-trans* conformation of the imine can be related to similar effects in the starting materials and product of the reaction, confirming that the steric interactions with the catalysts are probably not important in establishing the preference for the *S-cis* conformation. These effects might also be present in other reactions involving acyl imines.

The higher energy of the transition states in which the indole ring is not directed toward the acyl group (TS1-*E*-*s*-*cis*-ex, TS1-*E*-*s*-*trans*-ex, TS1-*Z*-*s*-*cis*-ex, TS1-*Z*-*s*-*trans*-ex, Scheme 1) shows the importance of the relative orientation of this group with respect to the imine. These two possible orientations initially lead to two diastereoisomers, as another chiral center is created in the indole ring. This chiral center is lost after the final tautomerization step as the indole ring recovers aromaticity, and so it is not possible to check the diastereomeric ratio obtained in the reaction. The transition state in which the indole ring is oriented toward the acyl group has a geometry more suitable for establishing interactions with the phosphoric acid catalyst (Figure 5). The distances between the imine and indole nitrogen atoms are shorter in this transition state (3.2 Å) and more similar to the distance between the phosphoric acid oxygen atoms (2.6 Å). This effect accounts for the major fraction of the overall stabilization of TS1-*E*-*s*-*cis*-end(*R*) over TS1-*E*-*s*-*cis*-ex(*S*), since calculations on the simplified 1,3 butadiene catalyst model affords a comparable energy difference (2.6 kcal/mol). The energy difference between TS1-*E*-*s*-*cis*-end(*R*) and TS1-*E*-*s*-*cis*-ex(*R*) is dominated mostly by steric effects.

Steric interactions are also responsible for the preference for TS1-*E*-*s*-*cis*-end(*R*) over TS1-*E*-*s*-*cis*-end (*S*). The bulky 2,4,6-triisopropyl phenyl groups of the catalyst have strong steric interactions with the imine and indole molecules in the transition state. Since the catalyst is chiral, these steric interactions are different for transition states leading to opposite enantiomers. A model similar to those shown in Figure 1, which was proposed to explain the enantioselectivity of the Strecker reaction on N-benzyl imines with the *E* conformation, can be employed in this reaction as well (Figure 6), but interactions with the large indole molecule become more relevant.

The indole ring is H-bonded to one of the phosphoric acid oxygen atoms. As the catalyst (anion) has a C_2 symmetry axis, equivalent results are obtained for both oxygens. In the most stable transition structures, the large indole molecule is directed to the side of the catalyst that is not occupied by the

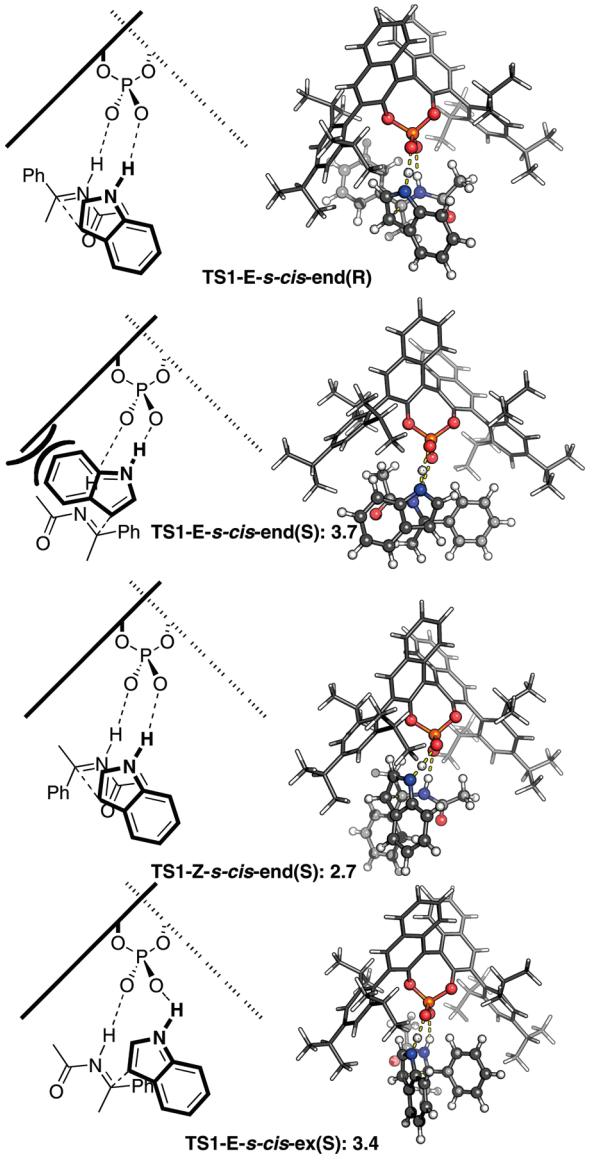

FIGURE 6. Transition structures found for Zhou's *N*-acylimine reaction. Atoms treated with the high level of theory are represented as ball-and-stick models, while atoms in the low-level layer are shown as a wire model.

bulky catalyst group, so steric interactions are minimized. The *E*-imine is bonded to the other oxygen atom of the phosphoric acid. In the most stable transition state (TS1-*E*-*s*-*cis*-end(*R*)), the acyl group is below the indole ring, since, as shown in Scheme 1 and Figure 6, in this orientation the phosphoric catalyst fits better to the transition state. In this conformation, the acyl group is directed toward the catalyst substituents, but steric interactions are reduced as the imine tilts with respect to the catalyst. This can be seen Scheme 1 and is particularly clear for TS1-*E*-*s*-*cis*-end(*S*), Figure 6.

A similar transition structure, Figure 6 TS1-*E*-*s*-*cis*-end-(*S*), in which the indole ring is directed to the other side of the catalyst has a higher energy, as does the structure TS1-*Z*-*s*-*cis*-end(*S*), in which the imine has the *Z* conformation. In TS1-*E*-*s*-*cis*-ex(*S*), the catalyst's bulky groups are directed away the indole ring but the indole−imine relative orientation is reversed. This change in the orientation forces a twist

SCHEME 2. Different Geometries of Transition Structures Studied for the *N*-Tosylimine Reactions[a]

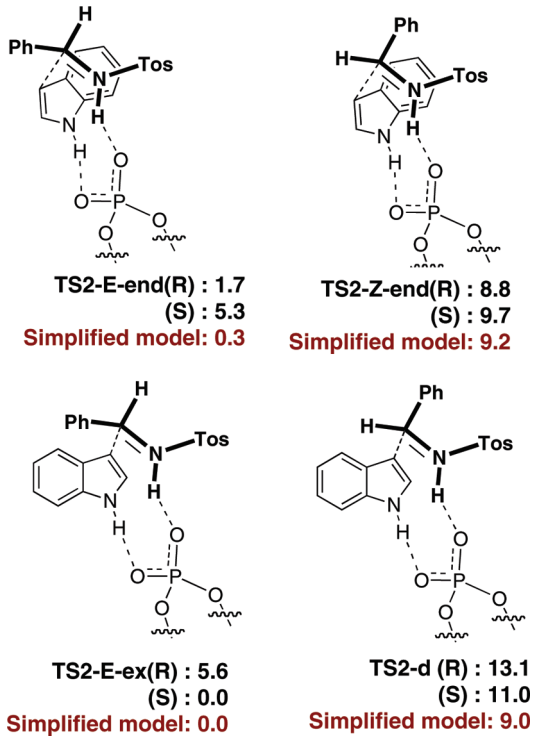

[a] $\Delta\Delta G$ (in toluene) are expressed in kcal/mol and refer to the use of the *R* catalyst.

in the imine and the indole around the C_2 catalyst symmetry axis, so H-bonds with phosphoric oxygens can be made. In TS1-*E*-*s*-*cis*-ex(*S*) the indole and the imine are sandwiched between the bulky catalyst substituents. This structure is destabilized as the orientation of the indole ring is disfavored.

Reaction between Indole and Tosylimines. You[64] has obtained good enantioselectivities using a 1-naphthyl-substituted BINOL−phosphoric acid catalyst for the Friedel−Crafts reaction of indole with the *N*-tosylimine derived from benzaldehyde, Figure 2. As in the previous study, the computational analysis has investigated the different geometric isomers (*Z* and *E*) of the imine and orientations of indole in the transition structures (catalyst's naphthyl rings were orientated to minimize steric interactions with the indole and the imine in the transition state; for TS2-*E*-end(*R*), as it was not clear which orientation would give smaller energy, an alternative geometry was calculated, resulting in a structure with 1.7 kcal/mol higher energy than the one shown) (Scheme 2). Considering the eight different transition structures, an 89% ee is calculated, and the major product shows *S* absolute configuration when the *R*-BINOL-derived catalysts is used. This is in good agreement with the experimental results (93% ee of the *R* product when *S* catalyst was employed).

As in the previous reaction, *E*-imine transition states (TS2-*E*-end and TS2-*E*-ex) are more stable than *Z*-imine transition states (TS2-*Z*-end and TS2-*Z*-ex), but in contrast to what we have found for *N*-acylimines, the most stable transition state corresponds to a structure in which the indole ring is not positioned over the *N*-tosyl group but over the acetophenone

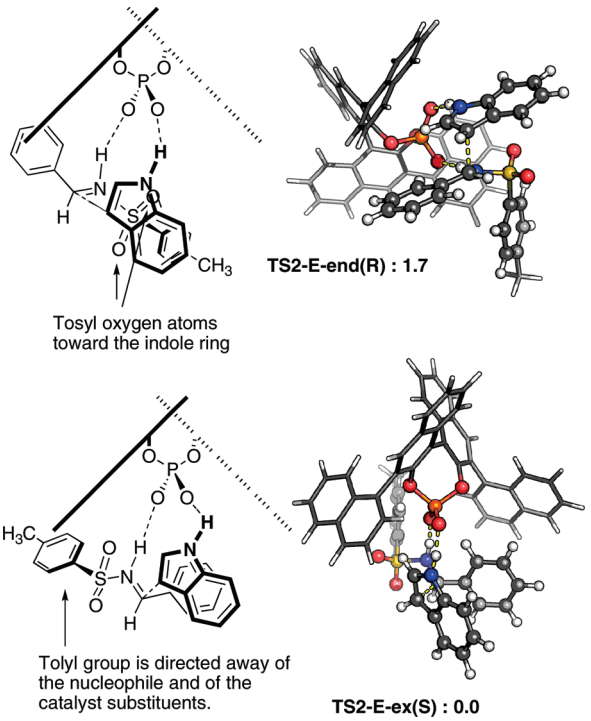

FIGURE 7. Two lowest energy transition structures for the *N*-tosylimine reaction. Atoms treated with the high level of theory are represented as ball-and-stick models, while atoms in the low-level layer are shown as a wire model.

phenyl ring. This change of conformation leads to the change in the absolute configuration of the preferred product. Similar transition states with the simplified catalyst model show similar Gibbs free energies: the transition state in which the indole ring is over the tosyl group is 0.3 kcal/mol more higher in energy, whereas in the *N*-acylimine reactions transition structures with this orientation were 1.9 and 2.6 kcal/mol more stable. This is probably a consequence of steric interactions between the tosyl oxygen atoms and the indole ring. These interactions compensate for the better fit of the structure to the phosphoric acid catalyst. Steric interactions with the naphthyl substituents of the catalyst are less important in the TS-2*E*-ex(*S*) transition state, since in this arrangement the indole and imine form a more compact structure.

The model to predict the absolute configuration is similar to that proposed for the reaction of *N*-benzylimines (Figure 7). The tosyl group is rotated around the N−S bond so the tolyl group is directed away from the nucleophile. In the most stable transition state diastereoisomer, the catalyst substituents avoid interactions with this group.

Conclusions

The good agreement between the calculated stereoinduction and the experimental results suggests that BINOL−phosphoric acid derivatives catalyze the Friedel−Crafts reaction of indole and *N*-acyl- or *N*-tosylimines by establishing simultaneous interactions with the electrophile and the nucleophile. The reaction mechanism, therefore, is similar to that found in the Hantzsch ester reduction of *N*-phenylimines[77] and to the Strecker reaction of benzylimines.[78] In addition, a similar model can be used to understand the

enantioselectivity of the BINOL-catalyzed reaction of enones with alkenyl borates,[88] indicating that the utility of these models might be general in reactions catalyzed by BINOL derivatives. The different conformations of the imine substrate and the orientation of the indole ring affects the relative energy of the transition structures, but these effects can be readily included in the analysis. For the reaction on *N*-acylimines, the most stable transition structures involve the *s-cis* acyl *E*-imine with the indole molecule positioned over the acyl group. The model used for predicting the enantioselective of other BINOL−phosphoric acid catalyzed reactions can also be employed here by placing the indole ring in the least sterically demanding position in the most stable transition state to minimize steric effects. In contrast, to the *N*-tosylimine reaction, the preferred orientation of the indole ring is reversed, and the model deduced from the study of the Strecker reaction on *N*-benzylimine can be used.[78] This change also explains the reversal in the stereoselectivity observed for the *N*-tosylimine reaction.

In summary, the enantioselectivity of the Friedel−Crafts reactions of indoles follows a scheme similar to that for other BINOL−phosphoric acid catalyzed reactions. The phosphoric acid coordinates to both nucleophile and electrophile, bringing them together in a chiral environment. The Friedel−Crafts reactions have an additional level of complexity over the reactions in our earlier studies: the large indole nucleophile prefers to attack the electrophile toward the edge of the chiral cavity. The absolute sense of stereoinduction can be explained using Figure 8.

Computational Methods

The need to calculate many transition structures and the high number of atoms of the catalyst does not allow the use of full QM methods. Instead, we have used hybrid QM/MM calculations. The ONIOM[89−91] method implemented in the Gaussian03 program[92] was used for geometry transition-state optimizations. The B3LYP functional[93] combined with the 6-31G* basis set[94−96] (augmented with polarization p functions for hydrogen atoms involved in bond-forming and -breaking processes) was used in the high level layer, and the low level layer was treated by the UFF[97] molecular mechanics force field. This combination has provided accurate geometries in previous studies of organocatalytic mechanisms.[77,78,98] The UFF force field is very suitable for the catalysts since it reproduces the DFT results for the energy of different dihedral angles in biphenyls.[77] In Figures 6 and 7, the layers are shown using different models: "ball and stick" model for the atoms included in the DFT layer and "wire" model for the atoms in the UFF layer; in Figure 9 the layers are shown in different colors. After geometry optimization, Gibbs free energy corrections to the energy are calculated at this level of theory, using the temperature employed in the experiments (273 K for the *N*-Boc benzaldehyde imine reaction and 298 K for the *N*-acetyl acetophenone imine reaction).

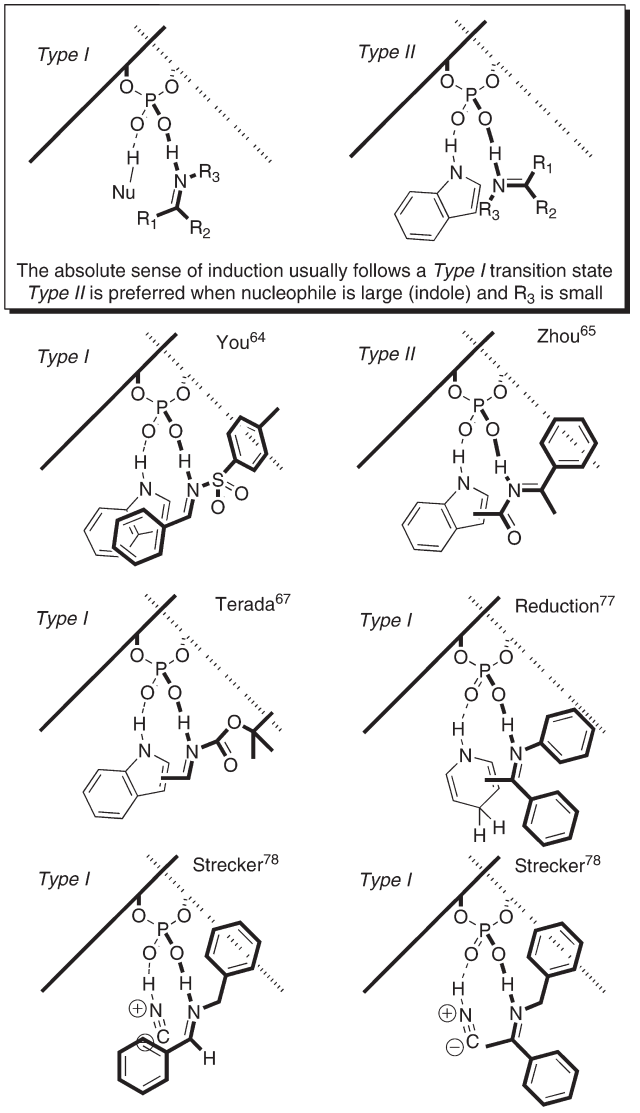

FIGURE 8. Model for the sense of stereoinduction in BINOL−phosphoric acid catalyzed reactions.

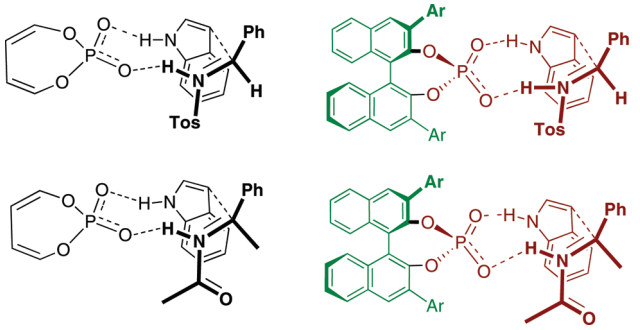

FIGURE 9. Simplified model of the transition-state structures (left) and distribution of atoms between high- and low-level layers in the ONIOM calculations (red, DFT layer; green, UFF layer).

(88) Paton, R. S.; Goodman, J. M.; Pellegrinet, S. C. *J. Org. Chem.* **2008**, *73*, 5078–5089.
(89) Svensson, M.; Humbel, S.; Morokuma, K. *J. Chem. Phys.* **1996**, *105*, 3654–3661.
(90) Vreven, T.; Morokuma, K. *J. Comput. Chem.* **2000**, *21*, 1419–1432.
(91) Dapprich, S.; Komaromi, I.; Byun, K. S.; Morokuma, K.; Frisch, M. J. *THEOCHEM* **1999**, 461–462.
(92) Frisch, M. J., et al. *Gaussian 03, Revision D.03*; Gaussian, Inc.: Wallingford, CT, 2004.
(93) Becke, A. D. *J. Chem. Phys.* **1983**, *98*, 5648–5652.
(94) Gill, P. M. W.; Johnson, B. G.; Pople, J. A.; Frisch, M. J. *Chem. Phys. Lett.* **1992**, *197*, 499–505.
(95) Krishnan, R.; Binkley, J. S.; Seeger, R.; Pople, J. A. *J. Chem. Phys.* **1980**, *72*, 650–654.
(96) Clark, T.; Chandrasekhar, J.; Schleyer, P. v. R. *J. Comput. Chem.* **1983**, *4*, 294–301.
(97) Rappé, A. K.; Casewit, C. J.; Colwell, K. S.; Goddard, W. A. III; Skid, W. M. *J. Am. Chem. Soc.* **1992**, *114*, 10024–10035.
(98) Simon, L.; Goodman, J. M. *Org. Biomol. Chem.* **2009**, *7*, 483–487.

For the resulting optimized structures, single-point energy was evaluated using the MPWB1K/6-31G** level of theory. This functional has been shown to give good results in describing weak nonbonded (dispersive) interactions.[99] Ultrafine grid and very tight SCF convergence criteria were used in this calculation. The effects of the solvent (toluene) used in the were included using the PCM[100−104] solvation model, with the cavity defined according to the UAKS[105] scheme. Gibbs free energy of each structure was obtained after adding the single-point energy and the Gibbs free energy correction calculated previously. The results obtained are in good agreement with the experimental values reported (94% ee for Zhou's reaction and 89% ee for You's reaction), regardless of the use of single-point MPWB1K/6-31G** (PCM) electronic energy (92% ee and 88% ee, respectively), zero-point corrected energy (97% ee and 88% ee), or Gibbs corrected energy (97% ee and 89% ee). Gibbs free energies have been used in the discussion, but no significant differences would be obtained if either electronic energy or zero-point energy was used.

The transition structures for the simplified model were optimized using full DFT calculations at the B3LYP/6-31G* level of theory. As in the ONIOM calculations, the basis set was extended by adding p polarization functions on the hydrogen atoms involved in the bond-forming and -breaking processes. Single-point energies were evaluated using MPWB1K/6-31G** level of theory. Calculations were performed in the gas phase to avoid the possible effect of different cavity geometries from the implicit solvation models, since these cavities will not resemble that ones in the full catalysts calculations. In the *N*-tosylimine reactions with the simplified model, the tosyl group was substituted by benzenosulfonyl group.

In order to test the ONIOM method, we reoptimized TS1-*E*-*scis*-end(*R*) and TS1-*Z*-*scis*-end(*S*) using the B3LYP functional and 6-31G* basis set and then carried out single-point energy evaluations using the MPWB1K/6-31G** functional and PCM (UAKS) solvation model for toluene. The single-point energy difference between the two reoptimized structures was 4.5 kcal/mol, which compares well with the 3.9 kcal/mol observed for the ONIOM-optimized structures.

Acknowledgment. This research was supported by a Marie Curie Intra-European Fellowship within the 6th European Community Framework Programme MEIF-CT2006-040554. We acknowledge the use of CamGrid service in carrying out this work and Dr. Charlotte Bolton for IT support.

Supporting Information Available: Complete list of authors in the Gaussian03 reference; Cartesian coordinates of optimized structures; comparison between ONIOM and full-DFT structures. This material is available free or charge via the Internet at http://pubs.acs.org.

(99) Zhao, Y.; Truhlar, D. G. *J. Chem. Theory Comput.* **2005**, *1*, 415–432.
(100) Cammi, R.; Mennucci, B.; Tomasi, J. *J. Phys. Chem. A* **2000**, *104*, 5631–5637.
(101) Cammi, R.; Mennucci, B.; Tomasi, J. *J. Phys. Chem. A* **1999**, *103*, 9100–9108.
(102) Cossi, M.; Rega, N.; Scalmani, M.; Barone, V. *J. Chem. Phys.* **2001**, *114*, 5691–5701.
(103) Cossi, M.; Scalmani, G.; Rega, N.; Barone, V. *J. Chem. Phys.* **2002**, *117*, 43–54.
(104) Cossi, M.; Scalmani, G.; Rega, N.; Barone, V. *J. Comput. Chem.* **2003**, *24*, 669–681.
(105) Barone, V.; Cossi, M.; Tomassi, J. *J. Chem. Phys.* **1997**, *107*, 3210–3221.